

Received:
14 May 2021Revised:
22 August 2021Accepted:
31 August 2021<https://doi.org/10.1259/bjr.20210601>

Cite this article as:

Ichikawa S, Motosugi U, Shimizu T, Kromrey ML, Aikawa Y, Tamada D, et al. Diagnostic performance and image quality of low-tube voltage and low-contrast medium dose protocol with hybrid iterative reconstruction for hepatic dynamic CT. *Br J Radiol* 2021; **94**: 20210601.

FULL PAPER

Diagnostic performance and image quality of low-tube voltage and low-contrast medium dose protocol with hybrid iterative reconstruction for hepatic dynamic CT

¹SHINTARO ICHIKAWA, MD, PhD, ^{1,2}UTAROH MOTOSUGI, MD, PhD, ¹TATSUYA SHIMIZU, MD, PhD,
^{1,3}MARIE LUISE KROMREY, MD, ⁴YOSHIHITO AIKAWA, RT, PhD, ¹DAIKI TAMADA, PhD and ¹HIROSHI ONISHI, MD, PhD

¹Department of Radiology, University of Yamanashi, 1110 Shimokato, Chuo, Yamanashi, Japan

²Department of Diagnostic Radiology, Kofu Kyoritsu Hospital, 1-9-1 Takara, Kofu, Yamanashi, Japan

³Department of Diagnostic Radiology and Neuroradiology, University Medicine Greifswald, Domstraße 11, Greifswald, Germany

⁴Division of Radiology, University of Yamanashi Hospital, 1110 Shimokato, Chuo, Yamanashi, Japan

Address correspondence to: Dr Shintaro Ichikawa
E-mail: shintaro@hama-med.ac.jp

Objective: To evaluate the diagnostic performance and image quality of the low-tube voltage and low-contrast medium dose protocol for hepatic dynamic CT.

Methods: This retrospective study was conducted between January and May 2018. All patients underwent hepatic dynamic CT using one of the two protocols: tube voltage, 80 kVp and contrast dose, 370 mgI/kg with hybrid iterative reconstruction or tube voltage, 120 kVp and contrast dose, 600 mgI/kg with filtered back projection. Two radiologists independently scored lesion conspicuity and image quality. Another radiologist measured the CT numbers of abdominal organs, muscles, and hepatocellular carcinoma (HCC) in each phase. Lesion detectability, HCC diagnostic ability, and image quality of the arterial phase were compared between the two protocols using the non-inferiority test. CT numbers and HCC-to-liver contrast were compared between the protocols using the Mann-Whitney *U* test.

Results: 424 patients (70.5 ± 10.1 years) were evaluated. The 80-kVp protocol showed non-inferiority in lesion

detectability and diagnostic ability for HCC (sensitivity, 85.7–89.3%; specificity, 96.3–98.6%) compared with the 120-kVp protocol (sensitivity, 91.0–93.3%; specificity, 93.6–97.3%) ($p < 0.001$ – 0.038). The ratio of fair image quality in the 80-kVp protocol also showed non-inferiority compared with that in the 120-kVp protocol in assessments by both readers ($p < 0.001$). HCC-to-liver contrast showed no significant differences for all phases ($p = 0.309$ – 0.705) between the two protocols.

Conclusion: The 80-kVp protocol with hybrid iterative reconstruction for hepatic dynamic CT can decrease iodine doses while maintaining diagnostic performance and image quality compared with the 120-kVp protocol.

Advances in knowledge: The 80- and 120-kVp protocols showed equivalent hepatic lesion detectability, diagnostic ability for HCC, image quality, and HCC-to-liver contrast.

The 80-kVp protocol showed a 38.3% reduction in iodine dose compared with the 120-kVp protocol.

INTRODUCTION

Hepatic dynamic CT with four phases—pre-contrast (pre-CT), arterial phase (AP), portal venous phase (PVP), and delayed phase (DP)—is widely used for routine detection and characterization of hepatic lesions. Hepatic lesions in high-risk patients that show typical CT findings of hepatocellular carcinoma (HCC) can be diagnosed as HCC without biopsy.¹ However, this technique involves radiation exposure and the use of a nephrotoxic iodine-based contrast medium (CM), which is a common cause of iatrogenic acute kidney injury.² Patients with chronic liver disease often share some risk factors for kidney injury, such

as advanced age and diabetes mellitus.³ Moreover, they require repeated hepatic dynamic CT scans for assessment of HCC development. Therefore, it is desirable to reduce the amount of CM used without causing a loss of image quality. Low-tube voltage CT is a well-established and effective method of reducing the contrast dose. Enhancement of iodine-based CM substantially increases at lower tube voltages, as the effective energy of the X-ray beam approaches the absorption k-edge of iodine (33.2 keV).⁴ Although lower tube voltages can increase the image noise because of the reduced number of X-ray photons, a compensatory increase in the tube current and the use of iterative

reconstruction (IR) instead of filtered back projection (FBP) can solve this problem.^{5,6} Currently, hybrid IR is the most popular IR method that implements a two-step noise reduction process, wherein streak artifacts are first removed from the projection data by combining the scanner model and the statistical noise model, and image reconstruction is then performed by FBP with repeated noise removal.⁷ This technique can improve image quality by decreasing image noise and artifacts in low-tube voltage hepatic dynamic CT.^{8,9} Nevertheless, although the utility of low tube voltage has been reported in multiple studies to date, the non-inferiority in the diagnostic performance of low-tube voltage dynamic liver CT has not been well clarified in comparison with standard-tube voltage CT.

We hypothesized that a protocol employing a low-tube voltage and low CM dose might be useful in routine practice because it could reduce the CM dose without causing a loss of image quality. The purpose of this study was to compare the diagnostic performance and image quality of a low-tube voltage (80 kVp) and low CM dose (370 mgI/kg) protocol with those of a conventional (120 kVp and 600 mgI/kg) protocol for hepatic dynamic CT.

METHODS AND MATERIALS

Patients

This single-center study was approved by the relevant institutional review board. The requirement for written informed consent was waived because this study retrospectively used the data from a clinical cohort. Between January and May 2018, 522 consecutive adult patients who underwent hepatic dynamic CT

were identified as eligible participants. From this population, the further selection was performed according to the following inclusion criteria: (i) body weight ≤ 75 kg, (ii) tube voltage and contrast dose, 120 kVp and 600 mgI/kg, respectively (120-kVp protocol) or 80 kVp and 370 mgI/kg, respectively (80-kVp protocol), and (iii) presence of available CT data.

CT and contrast medium injection protocols

The 80-kVp protocol CT was performed using a 320-detector-row unit, and the 120-kVp protocol CT was performed using a 64-detector-row unit because of a technical limitation. Patients with reduced renal function tended to be assigned to the 80-kVp protocol to reduce the dose of CM, while other patients were assigned to whichever protocol was available at the time of examination. The detailed scanning parameters of each protocol are shown in Table 1. Automatic exposure control (Real EC, Canon Medical Systems, Otawara, Japan) was used to optimize the dose for each patient. The maximum tube current was 580 mA with the 320-detector-row unit and 450 mA with the 64-detector-row unit. Therefore, we assumed that tube current would not be sufficient if the maximum tube currents of the CT units were used for the scan. A 370 mgI/kg or 600 mgI/kg dose of CM was intravenously administered using a power injector during a fixed injection time of 30 s.

Image reconstruction

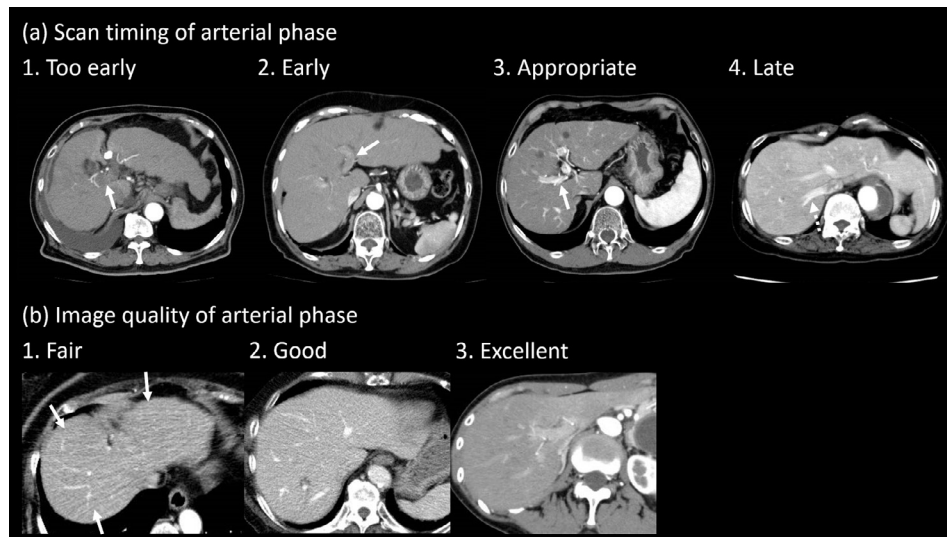
Image reconstruction was performed in a 32–45 cm display field of view, depending on the patient's physique. The 120-kVp images were reconstructed using a standard FBP algorithm with a standard soft tissue kernel (FC03). The 80-kVp images were

Table 1. Scanning parameters in each protocol

	80-kVp protocol	120-kVp protocol
CT unit	320-detector-row unit (Aquilion ONE; Canon Medical Systems, Otawara, Japan)	64-detector-row unit (Aquilion 64, Canon Medical Systems, Otawara, Japan)
Rotation time [s]	0.75	0.5
Beam collimation [mm]	80 × 0.5	64 × 0.5
Reconstructed section thickness [mm]	5	5
Reconstructed section interval [mm]	5	5
Helical pitch (beam pitch)	0.813	0.828
Table movement [mm/s]	43.6	52.9
Scanning field of view [cm]	40	40
Tube current [mA]	150–580	150–450
Effective mAs/slice	139–536	91–272
Total amount of contrast medium [mgI/kg]	370	600
Injection duration [s]	30	30
Scan delay after injection	Pre-contrast, 40 (AP), 70 (PVP), 180 (DP) s	Pre-contrast, 40 (AP), 70 (PVP), 180 (DP) s
Contrast medium	Iopamiron 370 (Iopamidol), Bayer Healthcare, Osaka, Japan; Iomeron 350 (Iomeprol), Eisai Co., Tokyo, Japan; Optiray 320 (Ioversol), Guerbet Japan, Tokyo, Japan or Omnipaque 300 (Iohexol), GE Healthcare Japan, Tokyo, Japan	

AP, arterial phase; PVP, portal venous phase; DP, delayed phase.

Figure 1. Examples of images with visual assessment. (a) Scan timing of the arterial phase was assessed using a 4-point scale (1, too early = without enhancement of the portal vein [arrow]; 2, early = weak enhancement of the portal vein [arrow]; 3, appropriate = adequate enhancement of the hepatic artery and portal vein [arrow] without enhancement of the hepatic vein; 4, late = enhancement of the hepatic vein [dotted arrow]). (b) Image quality of the arterial phase was assessed using a 3-point scale (1, fair = image noise or beam hardening artifacts [arrows] are present and slightly interfering with the depiction of intrahepatic structures; 2, good = image noise or beam hardening artifacts are present but not interfering with the depiction of intrahepatic structures; 3, excellent = minimal or no image noise or beam hardening artifacts).



reconstructed using the hybrid IR algorithm (adaptive iterative dose reduction [AIDR] 3D) and kernel FC03. The hybrid IR algorithm is a raw-data-based, statistical IR technique. During the reconstruction, a scanner model and a statistical noise model are considered to improve image quality and dose reduction.¹⁰ AIDR 3D is available at four strength levels (weak, mild, standard, and strong). The mild level was selected based on a previous study which reported half-dose CT scans compared to FBP can be achievable in small-sized patients without hampering diagnostic performance by applying the mild level of the hybrid IR.¹¹

Qualitative image analysis

One radiologist (S.I. with 11 years of experience in abdominal radiology) reviewed all images and chose slices of AP images with or without focal liver lesions from patients with focal liver lesions for evaluation. In patients with multiple lesions, the largest three lesions were selected for evaluation. For the remaining cases, slices of AP images for which the slice positions of liver CT were randomly chosen were selected for evaluation.

The AP images were independently and randomly assessed by two radiologists (S.I. and T.S. with 11 and 5 years of experience in abdominal radiology, respectively). They were unaware whether the patients had liver lesions or not. They evaluated the scan timing for AP images using a 4-point scale and the image quality of AP scans using a 3-point scale (Figure 1). The criteria of the scan timing were as follows: 1, too early = without enhancement of the portal vein; 2, early = weak enhancement of the portal vein; 3, appropriate = adequate enhancement of the hepatic artery and portal vein without enhancement of the hepatic vein; 4, late = enhancement of the hepatic vein. The criteria of the image quality were as follows: 1, fair = image noise or beam

hardening artifacts are present and slightly interfere with the depiction of intrahepatic structures; 2, good = image noise or beam hardening artifacts are present but do not interfere with the depiction of intrahepatic structures; 3, excellent = minimal or no image noise or beam hardening artifacts.

The radiologists were asked to detect any liver lesions for the assessment of lesion detectability. They were then required to identify HCCs among the lesions for the assessment of HCC diagnostic ability. These assessments were performed using a 5-point scale indicating the reviewers' confidence in diagnosing any hepatic lesion (including HCC and other lesions) as well as HCC in the slices by reviewing all the phases (1, hepatic lesion/HCC definitely absent; 2, hepatic lesion/HCC probably absent; 3, equivocal; 4, hepatic lesion/HCC probably present; and 5, hepatic lesion/HCC definitely present). Each radiologist used the LI-RADS v. 2018 criteria¹² for the assessment and assigned the scores based on their subjective judgments. Hypervascular pseudolesions and cysts were considered negative cases in the assessment of lesion detectability because they are not clinically significant. The radiologists could freely scroll all the AP images to evaluate pre-chosen slices and image quality.

Quantitative image analysis

Another radiologist (M.L.K. with 3 years of experience in abdominal radiology) measured the CT numbers of abdominal organs (liver, portal vein, abdominal aorta, pancreas, spleen, renal cortex, and renal medulla) and HCC in each phase for all patients by placing circular regions of interest (ROIs). Image noise was defined as the standard deviation of the ROI of the liver. To evaluate the contrast-to-noise ratio (CNR), we measured the attenuation of the erector spinae muscle. The contrast enhancement

(CE), CNR, and HCC-to-liver contrast were calculated using the following formulae:

$$CE \text{ of the organs or HCC} = \frac{CT \text{ number on each phase} - CT \text{ number on pre-contrast scan}}{SD \text{ of the liver}}$$

$$CNR \text{ of the organs or HCC} = \frac{(CT \text{ number of organs or HCC} - CT \text{ number of the erector spinae muscle})}{SD \text{ of the liver}}$$

HCC-to-liver contrast = CT number of HCC - CT number of the liver

Statistical analysis

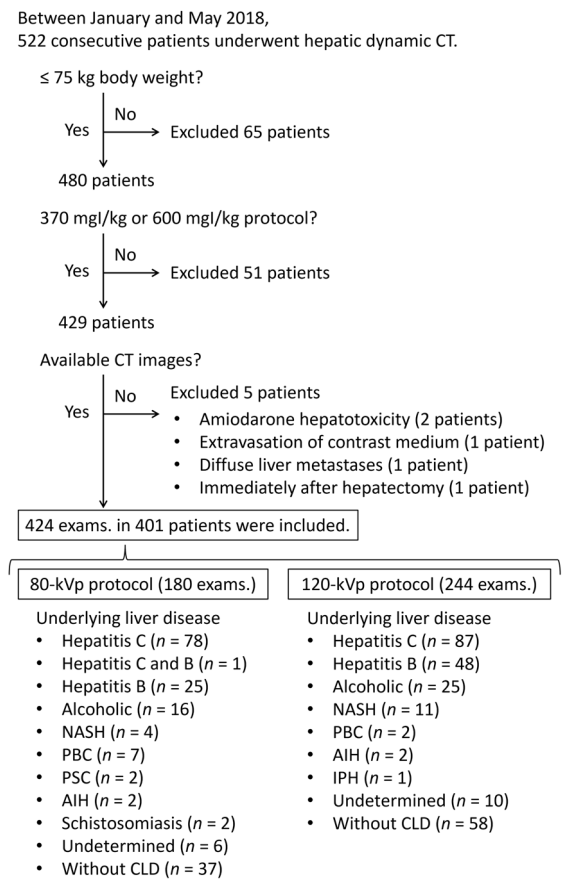
CM dose and injection rate and AP tube current were compared between the two protocols using the Mann-Whitney *U* test. Lesion detectability and diagnostic ability for HCC were evaluated in each protocol by calculating sensitivity, specificity, accuracy, positive and negative predictive values, and the area under the receiver operating characteristic curve (AUC). A score of ≥ 3 was considered to indicate a positive result. Non-inferiority of AP image quality, lesion detectability, and diagnostic ability for HCC of the 80-kVp protocol were compared with those of the 120-kVp protocol using a one-sided χ^2 test with a 7.5% non-inferiority margin. The non-inferiority of the AUC of the 80-kVp protocol was compared with that of the 120-kVp protocol using a one-sided Student's *t*-test with a 7.5% non-inferiority margin.¹³ Prior non-inferiority tests on diagnostic imaging have reported margins of 6–10%^{14–16}; thus, in this study, the margin was set at 7.5%, which was within this range. Weighted κ values were calculated to assess interobserver agreement. Agreement was considered excellent for κ values (κ) >0.8 , good for $0.6 < \kappa \leq 0.8$, moderate for $0.4 < \kappa \leq 0.6$, fair for $0.2 < \kappa \leq 0.4$, and poor for $\kappa \leq 0.2$. All statistical analyses were performed using JMP software (v. 14.1.0; SAS Institute Inc., Cary, NC) and R (v. 3.6.2; The R Foundation for Statistical Computing, Vienna, Austria). *p*-values <0.05 were considered statistically significant.

RESULTS

Patient demographics for each protocol

The final study cohort consisted of 401 patients (mean age, 70.5 ± 10.2 [range, 33–91] years) and included 270 men (71.1 ± 9.6 [40–91] years) and 131 women (69.4 ± 11.3 [33–91] years). Patients who underwent both protocols during the study period were included in both protocols; therefore, 424 examinations were included. Of these, 180 examinations were scanned using the 80-kVp protocol, and 244 examinations underwent the 120-kVp protocol. Based on the exclusion criteria, 121 patients were excluded (Figure 2). The underlying liver diseases in patients in the final study cohort are shown in Figure 2. A significant difference between the protocols was observed in age and estimated glomerular filtration rate (eGFR) ($p = 0.010$ and 0.027 , respectively). Other factors, including sex, body weight, body mass index, presence or absence of chronic liver disease, history of liver surgery or liver lesion, and lesion size, did not show significant differences between the protocols ($p = 0.251$ – 0.604 , Table 2).

Figure 2. Flowchart of patient enrollment between January and May 2018, 522 consecutive adult patients who underwent hepatic dynamic CT were identified as eligible participants. From this population, 121 patients were excluded based on the exclusion criteria. Therefore, the final study cohort consisted of 401 patients. Patients who underwent both protocols during the study period were included in both protocols; therefore, 424 examinations were included. Of these, 180 examinations were scanned using the 80-kVp protocol, and 244 examinations underwent the 120-kVp protocol. AIH, autoimmune hepatitis; CLD, chronic liver disease; IPH, idiopathic portal hypertension; exams., examinations; NASH, nonalcoholic steatohepatitis; PBC, primary biliary cholangitis; PSC, primary sclerosing cholangitis.



Evaluated hepatic lesions

278 slices (235 slices with focal liver lesions and 43 slices without focal liver lesions) were chosen from 146 examinations with focal liver lesions. From the rest of the cases, 345 slices were selected. In total, 623 slices of AP images (265 slices from the 80-kVp protocol and 358 slices from the 120-kVp protocol) were selected from 424 examinations for evaluation (Figure 3). Final diagnoses of 623 slices were as follows; HCC, $n = 116$ (mean size, 14.4 ± 7.5 [range, 5–40] mm); other liver tumors, $n = 119$ (17.0 ± 9.9 [5–50] mm); hypervascular pseudolesions, $n = 78$; cysts, $n = 97$; and no lesion, $n = 213$ (Figure 3). 29 lesions were pathologically confirmed, while the remaining lesions were diagnosed using imaging and clinical observation. The detailed criteria for the

Table 2. Patient demographics in each protocol

Variables	80-kVp protocol	120-kVp protocol	p-value
Number of examinations	180	244	-
Age [years]	71.7 ± 10.4	69.6 ± 9.7	0.010*
Sex [male: female]	126:54	163:81	0.527
Body weight [kg]	57.0 ± 9.0	58.1 ± 9.8	0.251
Body mass index [kg/m ²]	22.5 ± 3.1	22.8 ± 3.3	0.317
Chronic liver disease [present: absent]	143:37	186:58	0.480
History of liver surgery [present: absent]	42:138	51:193	0.555
eGFR [mL/min/1.73 m ²]	68.6 ± 17.0	72.0 ± 16.8	0.027*
Liver lesionb [present: absent]	64:116	81:163	0.604
Lesion size [mm]	15.4 ± 9.5	14.4 ± 7.9	0.477

eGFR, estimated glomerular filtration rate.

Continuous variables were analyzed by Wilcoxon test and are expressed as mean ± standard deviation. Categorical variables were analyzed by the χ^2 test and are expressed as ratios.

* $p < 0.05$

^bExcept for cyst and hypervascular pseudolesions

imaging and clinical observation-based diagnoses are described in [Supplementary Material 1](#).

Dose and injection rate of CM and tube current for the AP in each protocol

The CM volume, iodine dose, and injection rate in the 80-kVp protocol were significantly lower than those in the 120-kVp protocol (all $p < 0.001$). Tube current in the 80-kVp protocol was significantly higher than that in the 120-kVp protocol ($p < 0.001$). The proportion of cases showing insufficient tube current was not significantly different between the two protocols ($p = 0.410$) (Table 3).

Qualitative image analysis

Both readers noted non-inferiority in the proportions of appropriate scan timing of AP and the proportion of fair image quality in the 80-kVp protocol in comparison with the 120-kVp protocol ($p < 0.001$) (Table 3).

Lesion detectability and diagnostic ability for HCC of both protocols and readers were high (sensitivity, 85.7–93.3%; specificity, 93.6–98.6%; AUC, 0.93–0.96) (Table 4). All parameters of lesion detectability and diagnostic ability for HCC in the 80-kVp protocol showed non-inferiority in comparison with those in the 120-kVp protocol ($p < 0.001$ –0.039) (Table 4). Interobserver

Figure 3. Breakdown of evaluated hepatic lesions. 278 slices (235 slices with focal liver lesions and 43 slices without focal liver lesions) from 146 examinations with focal liver lesions were selected for the evaluation. In patients with multiple lesions, the three largest lesions were selected for analysis. From the rest of the cases, 345 slices were selected for which the slice positions in liver CT were randomly chosen. In total, 623 slices of arterial phase images (265 slices from the 80-kVp protocol and 358 slices from the 120-kVp protocol) were obtained from 424 examinations for evaluation. APHE, arterial phase hyperehancement; exams., examinations; FLLs, focal liver lesions; HBP, hepatobiliary phase; HCC, hepatocellular carcinoma; FNH, focal nodular hyperplasia.

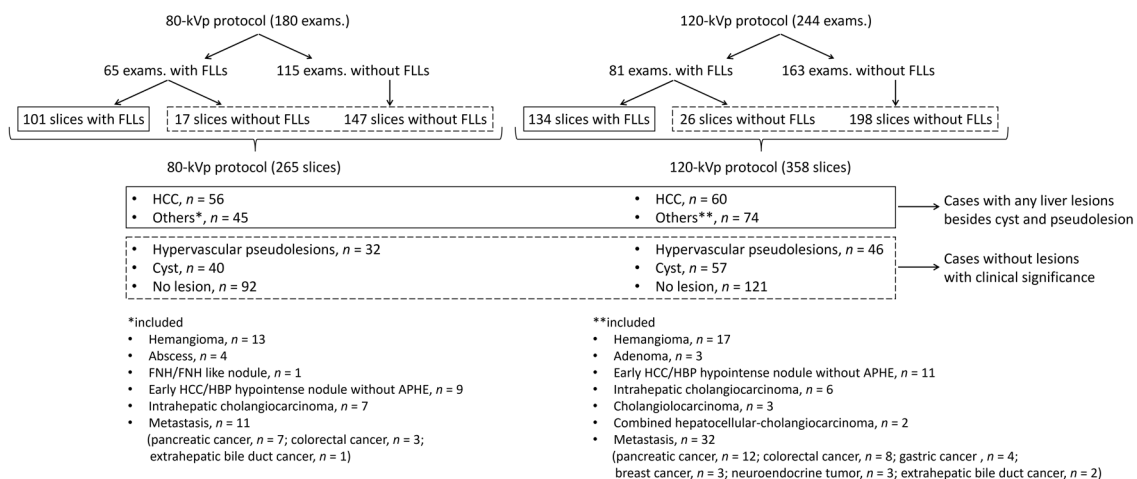


Table 3. Contrast medium injection parameters, tube current, and image quality in each protocol

Variables	80-kVp protocol	120-kVp protocol	P value
Injection condition of contrast medium			
Volume of contrast medium [mL]	63.5 ± 10.3	101.5 ± 17.1	<0.001*
Iodine dose [g]	20.9 ± 3.3	34.9 ± 5.9	<0.001*
Injection rate [mL/s]	2.1 ± 0.3	3.4 ± 0.5	<0.001*
Tube current			
Tube current [mA]	541.9 ± 45.4	390.6 ± 63.1	<0.001*
Insufficient tube current	36.7% (66/180)	32.8% (80/244)	0.410
Image quality of arterial phase			
Appropriate scan timing (Reader 1)	83.9% (151/180)	82.0% (200/244)	<0.001*
Appropriate scan timing (Reader 2)	80.6% (145/180)	81.6% (199/244)	<0.001*
Fair image quality (Reader 1)	1.7% (3/180)	0.4% (1/244)	<0.001*
Fair image quality (Reader 2)	2.2% (4/180)	0.8% (2/244)	<0.001*

Contrast medium injection parameters and tube current were analyzed by Wilcoxon test and are expressed as mean ± standard deviation. Non-inferiority of image quality in the arterial phase in the 80-kVp protocol was compared to those in the 120-kVp protocol by one-sided χ^2 test with 7.5% non-inferiority margin.

Categorical variables are expressed as ratios or percentage with numerators and denominators.

*p < 0.05

agreements were good for the scan timing and image quality of AP (80-kVp and 120-kVp, $\kappa = 0.73$ [95% CI, 0.65–0.81] and 0.72 [0.65–0.79], respectively) and excellent for the scores of the confidence of the presence of hepatic lesions and HCCs ($\kappa = 0.86$ [0.82–0.90] and 0.86 [0.81–0.90], respectively).

Case examples are shown in Figures 4 and 5. Figure 4 shows the findings for a patient with HCC who underwent both 80-kVp and 120-kVp protocols with a 10 day interval, while Figure 5 shows the findings for a patient with intrahepatic cholangiocarcinoma who underwent both 80-kVp and 120-kVp protocols

Table 4. Lesion detectability and diagnostic ability for hepatocellular carcinoma in each protocol

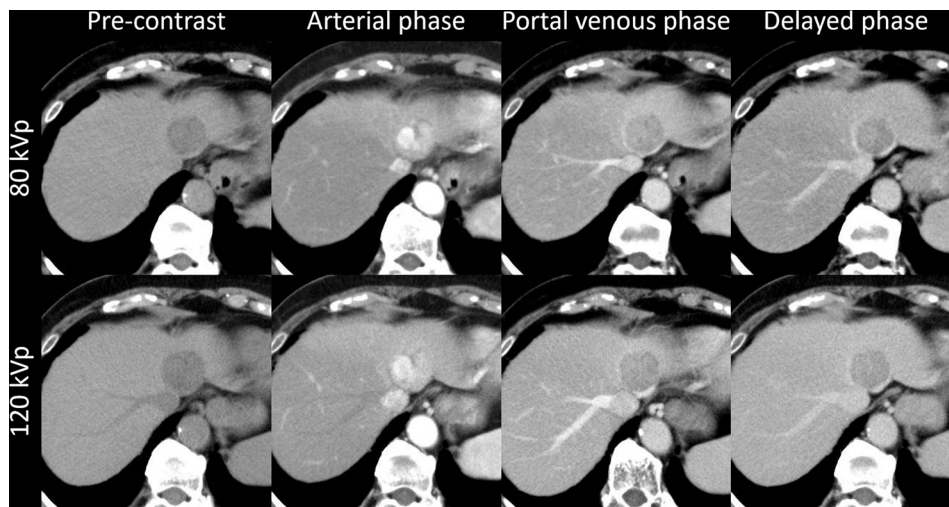
	Reader 1			Reader 2		
	80-kVp protocol	120-kVp protocol	P value	80-kVp protocol	120-kVp protocol	P value
Lesion detectability						
Sensitivity	89.1% (90/101)	91.0% (122/134)	<0.001a	86.1% (87/101)	92.5% (124/134)	<0.001a
Specificity	96.3% (158/164)	97.3% (218/224)	<0.001a	97.0% (159/164)	94.6% (212/224)	<0.001a
Accuracy	93.6% (248/265)	95.0% (340/358)	<0.001a	92.8% (246/265)	93.9% (336/358)	<0.001a
Positive predictive value	93.8% (90/96)	95.3% (122/128)	<0.001a	94.6% (87/92)	91.2% (124/136)	<0.001a
Negative predictive value	93.5% (158/169)	94.8% (218/230)	<0.001a	91.9% (159/173)	95.5% (212/222)	<0.001a
Area under the curve	0.93 (0.89–0.96)	0.95 (0.92–0.97)	0.018a	0.93 (0.89–0.96)	0.95 (0.92–0.97)	0.012a
Diagnostic ability for hepatocellular carcinoma						
Sensitivity	89.3% (50/56)	93.3% (56/60)	<0.001a	85.7% (48/56)	91.7% (55/60)	0.038a
Specificity	98.6% (206/209)	97.0% (289/298)	<0.001a	98.6% (206/209)	93.6% (279/298)	<0.001a
Accuracy	96.6% (256/265)	96.4% (345/358)	<0.001a	95.8% (254/265)	93.3% (334/358)	<0.001a
Positive predictive value	94.3% (50/53)	86.2% (56/65)	<0.001a	94.1% (48/51)	74.3% (55/74)	<0.001a
Negative predictive value	97.2% (206/212)	98.6% (289/293)	<0.001a	96.3% (206/214)	98.2% (279/284)	<0.001a
Area under the curve	0.94 (0.88–0.97)	0.96 (0.91–0.98)	0.039a	0.94 (0.88–0.97)	0.96 (0.91–0.98)	0.036a

Non-inferiority of sensitivity, specificity, accuracy, and positive/negative predictive values of the 80-kVp protocol were compared to those in the 120-kVp protocol by one-sided χ^2 test with a 7.5% non-inferiority margin. Area under the curve of the 80-kVp protocol was compared to those of 120-kVp protocol by one-sided Student's *t*-test with a 7.5% non-inferiority margin.

Categorical variables are expressed as percentage with numerators and denominators.

^aP < 0.05

Figure 4. A patient with HCC. A 73-year-old female with hepatitis B had HCC (31mm) at S3. This patient underwent both the 80-kVp and 120-kVp protocols with a 10 day interval. This lesion showed non-rim arterial phase hyperenhancement and non-peripheral washout on portal venous/delayed phases. These findings and the image quality are equivalent in both protocols. HCC, hepatocellular carcinoma.



with a 2 month interval. Both protocols showed similar image quality and typical imaging findings of HCC and intrahepatic cholangiocarcinoma.

Quantitative image analysis

The image noise in each phase was significantly lower for the 80-kVp protocol than for the 120-kVp protocol (80-kVp protocol vs 120-kVp protocol on pre-contrast scan, 9.1 ± 1.7 vs. 9.7 ± 1.5 [$p < 0.001$]; AP, 9.7 ± 1.8 vs. 10.3 ± 1.7 [$p = 0.001$]; PVP, 10.0 ± 2.0 vs. 10.5 ± 1.8 [$p = 0.002$]; DP, 9.8 ± 1.8 vs. 10.2 ± 1.7 [$p = 0.013$]).

The mean CT numbers of the liver, portal vein, abdominal aorta, pancreas, spleen, renal cortex, renal medulla, and HCC

on pre-CT were significantly higher for the 80-kVp protocol than for the 120-kVp protocol ($p < 0.001$ – 0.034) (Supplementary Material 1 and Figure 6). The CE of the abdominal aorta on AP, PVP, and DP; portal vein on PVP and DP; spleen on PVP and DP; renal cortex on AP, PVP, and DP; and renal medulla on DP were significantly higher for the 80-kVp protocol than for the 120-kVp protocol ($p < 0.001$ – 0.002) (Supplementary Material 1). The CNR of the liver on PVP; portal vein on pre-CT, PVP, and DP; abdominal aorta for all phases; pancreas on AP and PVP; spleen on pre-CT, PVP, and DP; renal cortex on AP, PVP, and DP; and renal medulla on PVP and DP were significantly higher for the 80-kVp protocol than for the 120-kVp protocol ($p < 0.001$ – 0.042) (Supplementary Material 1).

Figure 5. A patient with ICC. A 66-year-old female with primary sclerosing cholangitis had ICC (40 mm) at S4. This patient underwent both the 80-kVp and 120-kVp protocols with a 2 month interval. This lesion showed rim arterial phase hyperenhancement and delayed central enhancement. These findings and the image quality are equivalent in both protocols. ICC, intrahepatic cholangiocarcinoma.

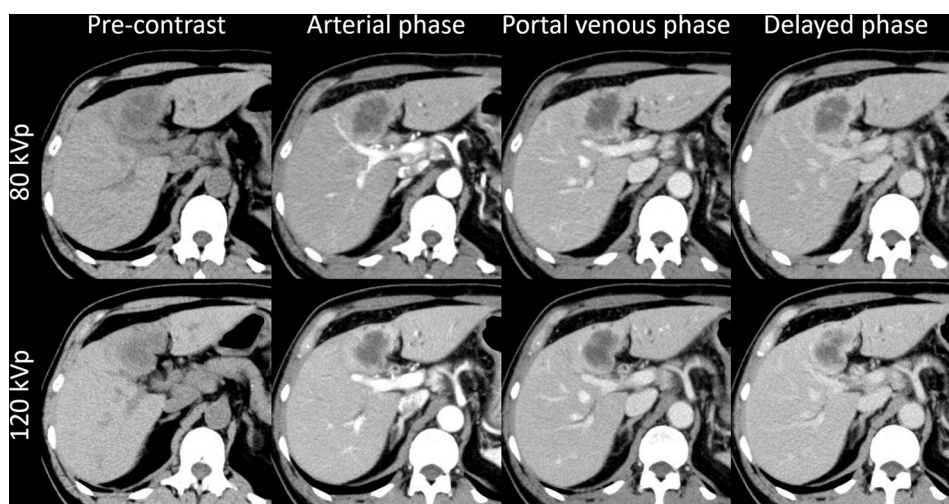
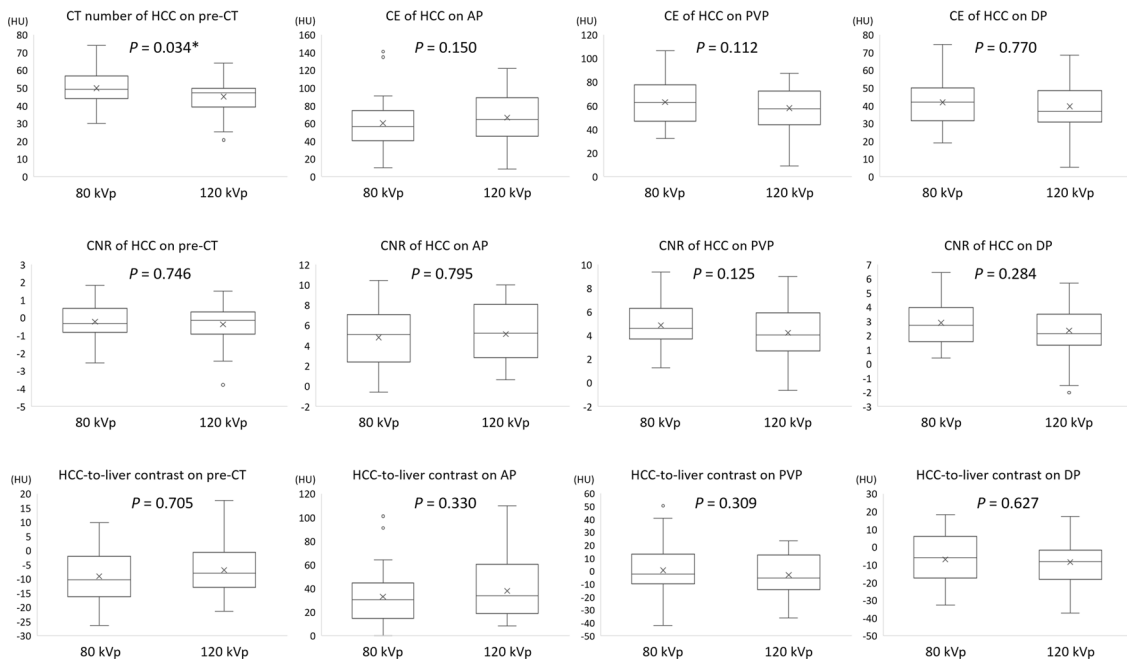


Figure 6. Box plots of the CT number of HCC on pre-contrast CT, CE of HCC, CNR, and HCC-to-liver contrast for each phase CT number of HCC for the 80-kVp protocol was significantly higher than that for the 120-kVp protocol on the pre-contrast scan ($p = 0.034$). In contrast, the CE of HCC, CNR of HCC, and HCC-to-liver contrast were not significantly different for all phases ($p = 0.112$ – 0.795). Note: The body of the boxplot consists of a box, which goes from the first quartile (Q1) to the third quartile (Q3). Within the box, a horizontal line is drawn at the median and a cross-mark is drawn at the mean of the dataset. The vertical lines are drawn at the smallest and largest data points, except for outliers. Outliers are drawn as circles. AP, arterial phase; CE, contrast enhancement; CNR, contrast-to-noise ratio; DP, delayed phase; HCC, hepatocellular carcinoma; HU, Hounsfield unit; pre-CT, pre-contrast CT; PVP, portal venous phase.



The CT number of HCC in the 80-kVp protocol was significantly higher than that in the 120-kVp protocol on pre-CT ($p = 0.034$). In contrast, the CE of HCC, CNR of HCC, and HCC-to-liver contrast were not significantly different for all phases between the two protocols ($p = 0.112$ – 0.795) (Figure 6).

DISCUSSION

Our results demonstrated that in comparison with the 120-kVp protocol, the 80-kVp protocol with a reduced iodine dose showed non-inferiority in image quality, lesion detectability, and diagnostic ability for HCC. CNR of HCC and HCC-to-liver contrast did not significantly differ for all phases between the two protocols. These results will facilitate the routine use of the low-tube voltage protocol in patients with liver diseases in order to reduce the iodine dose.

Low-tube voltage hepatic dynamic CT shows high diagnostic ability for HCC,^{17–19} with the sensitivity, specificity, accuracy, and AUC for HCC diagnosis being 82–100%, 97–100%, 77–80%, and 0.94–0.99, respectively. Our results corresponded to those findings. In general, specificity is important for HCC diagnosis, and low-tube voltage hepatic dynamic CT showed high specificity. Thus, low-tube voltage hepatic dynamic CT is useful because of the considerable increases in hepatic enhancement and HCC conspicuity with lower radiation and CM doses. The quantitative image quality in previous reports focused on the diagnostic ability for HCC. We also investigated lesion detectability in the two protocols, and low-tube voltage hepatic dynamic CT showed

high lesion detectability not only for HCC but also other hepatic lesions, while its ability was not inferior to that of the standard protocol. This is a new finding shown in our study.

Enhancement of iodine-based CM is known to substantially increase at lower tube voltages, but its effects on the CT numbers of abdominal organs on pre-contrast images have not been clarified. Our study revealed that the mean CT numbers of the liver, portal vein, abdominal aorta, pancreas, spleen, renal cortex, renal medulla, and HCC on pre-contrast CT were significantly higher for the 80-kVp protocol than for the 120-kVp protocol. In contrast, Sun et al reported no significant differences in the mean CT numbers of abdominal organs between the 100-kVp and 120-kVp protocols by using dual-source CT.²⁰ However, they used the same CT machine for both 100- and 120-kVp protocols, while we used two different CT machines for the 80- and 120-kVp protocols. This may have influenced the differences in the results. After CM administration, the CE and CNR were significantly higher for the 80-kVp protocol than for the 120-kVp protocol for most organs in each phase. These results suggest that the 80-kVp protocol can yield better contrast despite the smaller amount of CM than the 120-kVp protocol. In contrast, the CE of HCC, CNR of HCC, and HCC-to-liver contrast of the two protocols were not significantly different for all phases. Although our results corresponded to some previous reports,^{18,21–23} they also differed from others.^{8,9,17,24–26} These differences may be caused by slight variations in the amount of CM administered and the scanning parameters. Further studies are needed to determine

the optimal settings of low-tube voltage CT for hepatic dynamic CT.

Low-tube voltage CT is an effective method to reduce the CM dose. Patients with chronic liver disease often share some risk factors for kidney injury, such as advanced age and diabetes mellitus³; therefore, protocols with low CM doses are desirable to reduce the iodine burden in kidneys.

Our study had some limitations. First, the lack of histopathological confirmation for a large number of evaluated hepatic lesions is a potential limitation of this study. Second, the range and mean values of body weights of our patients were relatively smaller than those of North American and European individuals. In patients with large bodies, low-tube voltage scans tend to show poorer image quality due to the increased image noise attributable to radiation scattering and absorption. Thus, further studies are needed to determine whether our results are applicable for cohorts with higher body weights. Third, radiation doses between the two protocols were not comparable because the two CT units displayed the volume CT dose index differently (maximum in 120-kVp protocol [CT dose index, 32.1 ± 9.3 mGy; dose-length product, 880.2 ± 312.0 mGy-cm] vs average in 80-kVp protocol [CT dose index, 15.1 ± 3.6 mGy; dose-length product, $397.3 \pm$

121.8 mGy-cm]). However, phantom scans (Appendix 3) can be an alternative method for showing differences in the radiation doses for the two protocols. Fourth, about one-third of cases (36.7% [66/180] in 80-kVp protocol and 32.8% [80/244] in 120-kVp protocol) showed insufficient tube current. Finally, significant differences in age and estimated glomerular filtration rate were observed between the 80- and 120-kVp protocols due to the retrospective study design. Renal insufficiency tends to occur in patients with advanced age. However, the effects of age and renal function on our study's findings were minimal because the major factors affecting CE (iodine dose and injection methods) were well controlled in the protocols.

In summary, the 80-kVp protocol with hybrid IR for hepatic dynamic CT can decrease iodine doses while maintaining diagnostic performance and image quality in comparison with the 120-kVp protocol.

CONFLICT OF INTEREST

The authors declare that they have no conflict of interest.

FUNDING

This research did not receive any specific grant from funding agencies in the public, commercial, or not-for-profit sectors.

REFERENCES

- Marrero JA, Kulik LM, Sirlin CB, Zhu AX, Finn RS, Abecassis MM, et al. Diagnosis, staging, and management of hepatocellular carcinoma: 2018 practice guidance by the American association for the study of liver diseases. *Hepatology* 2018; **68**: 723–50. doi: <https://doi.org/10.1002/hep.29913>
- Mohammed NMA, Mahfouz A, Achkar K, Rafie IM, Hajar R. Contrast-Induced nephropathy. *Heart Views* 2013; **14**: 106–16. doi: <https://doi.org/10.4103/1995-705X.125926>
- Desbois A-C, Cacoub P, mellitus D. Diabetes mellitus, insulin resistance and hepatitis C virus infection: a contemporary review. *World J Gastroenterol* 2017; **23**: 1697–711. doi: <https://doi.org/10.3748/wjg.v23.i9.1697>
- Szucs-Farkas Z, Verdun FR, von Allmen G, Mini RL, Vock P. Effect of X-ray tube parameters, iodine concentration, and patient size on image quality in pulmonary computed tomography angiography: a chest-phantom-study. *Invest Radiol* 2008; **43**: 374–81. doi: <https://doi.org/10.1097/RLI.0b013e3181690042>
- Beister M, Kolditz D, Kalender WA. Iterative reconstruction methods in X-ray CT. *Phys Med* 2012; **28**: 94–108. doi: <https://doi.org/10.1016/j.ejmp.2012.01.003>
- Solomon J, Marin D, Roy Choudhury K, Patel B, Samei E. Effect of radiation dose reduction and reconstruction algorithm on image noise, contrast, resolution, and detectability of subtle hypoattenuating liver lesions at multidetector CT: filtered back projection versus a commercial model-based iterative reconstruction algorithm. *Radiology* 2017; **284**: 777–87. doi: <https://doi.org/10.1148/radiol.2017161736>
- Stiller W. Basics of iterative reconstruction methods in computed tomography: a vendor-independent overview. *Eur J Radiol* 2018; **109**: 147–54. doi: <https://doi.org/10.1016/j.ejrad.2018.10.025>
- Nakaura T, Nakamura S, Maruyama N, Funama Y, Awai K, Harada K, et al. Low contrast agent and radiation dose protocol for hepatic dynamic CT of thin adults at 256-detector row CT: effect of low tube voltage and hybrid iterative reconstruction algorithm on image quality. *Radiology* 2012; **264**: 445–54. doi: <https://doi.org/10.1148/radiol.12111082>
- Taguchi N, Oda S, Utsunomiya D, Funama Y, Nakaura T, Imuta M, et al. Using 80 kVp on a 320-row scanner for hepatic multiphasic CT reduces the contrast dose by 50 % in patients at risk for contrast-induced nephropathy. *Eur Radiol* 2017; **27**: 812–20. doi: <https://doi.org/10.1007/s00330-016-4435-y>
- Willeminck MJ, de Jong PA, Leiner T, de Heer LM, Nievelstein RAJ, Budde RPJ, et al. Iterative reconstruction techniques for computed tomography Part 1: technical principles. *Eur Radiol* 2013; **23**: 1623–31. doi: <https://doi.org/10.1007/s00330-012-2765-y>
- Yoon JH, Lee JM, Hur BY, Baek J, Shim H, Han JK, et al. Influence of the adaptive iterative dose reduction 3D algorithm on the detectability of low-contrast lesions and radiation dose repeatability in abdominal computed tomography: a phantom study. *Abdom Imaging* 2015; **40**: 1843–52. doi: <https://doi.org/10.1007/s00261-014-0333-4>
- American College of Radiology Committee on LI-RADS®. CT/MRI LI-RADS® v2018 Core.. Available from: <https://www.acr.org/-/media/ACR/Files/RADS/LI-RADS/LI-RADS-2018-Core.pdf> [Accessed on July 12, 2021].
- Zhou XH, Obuchowski NA, McClish DK. *Statistical Methods in Diagnostic Medicine*. Second Edition. New York, NY: Wiley; 2002. pp. 189–92.
- Lanotte SJ, Larbi A, Michoux N, Baron M-P, Hamard A, Mourad C, et al. Value of CT to detect radiographically occult injuries of the proximal femur in elderly patients after low-energy trauma: determination of non-inferiority margins of CT in comparison

- with MRI. *Eur Radiol* 2020; **30**: 1113–26. doi: <https://doi.org/10.1007/s00330-019-06387-2>
15. Xin Y, Zhang X, Yang Y, Chen Y, Wang Y, Zhou X, et al. A multicenter, hospital-based and non-inferiority study for diagnostic efficacy of automated whole breast ultrasound for breast cancer in China. *Sci Rep* 2021; **11**: 13902. doi: <https://doi.org/10.1038/s41598-021-93350-1>
 16. Tiegs-Heiden CA, Adkins MC, Carter RE, Geske JR, McKenzie GA, Ringler MD. Does gadolinium improve magnetic resonance arthrography of the hip beyond fluid distension alone? *Clin Radiol* 2020; **75**: 713.e1–713.e9. doi: <https://doi.org/10.1016/j.crad.2020.01.019>
 17. Pregler B, Beyer LP, Teufel A, Niessen C, Stroszczyński C, Brodoefel H, et al. Low tube voltage liver MDCT with sinogram-affirmed iterative reconstructions for the detection of hepatocellular carcinoma. *Sci Rep* 2017; **7**: 9460. doi: <https://doi.org/10.1038/s41598-017-10095-6>
 18. Noda Y, Kanematsu M, Goshima S, Kondo H, Watanabe H, Kawada H, et al. Reducing iodine load in hepatic CT for patients with chronic liver disease with a combination of low-tube-voltage and adaptive statistical iterative reconstruction. *Eur J Radiol* 2015; **84**: 11–18. doi: <https://doi.org/10.1016/j.ejrad.2014.10.008>
 19. Lee CH, Kim KA, Lee J, Park YS, Choi JW, Park CM. Using low tube voltage (80kVp) quadruple phase liver CT for the detection of hepatocellular carcinoma: two-year experience and comparison with Gd-EOB-DTPA enhanced liver MRI. *Eur J Radiol* 2012; **81**: e605–11. doi: <https://doi.org/10.1016/j.ejrad.2011.12.033>
 20. Sun H, Xue H-dan, Jin Z-yu, Wang X, Chen Y, He Y-lan, et al. Non-enhanced low-tube-voltage high-pitch dual-source computed tomography with sinogram affirmed iterative reconstruction algorithm of the abdomen and pelvis. *Chin Med Sci J* 2014; **29**: 214–20. doi: [https://doi.org/10.1016/S1001-9294\(14\)60073-0](https://doi.org/10.1016/S1001-9294(14)60073-0)
 21. Nakaura T, Awai K, Oda S, Funama Y, Harada K, Uemura S, et al. Low-kilovoltage, high-tube-current MDCT of liver in thin adults: pilot study evaluating radiation dose, image quality, and display settings. *AJR Am J Roentgenol* 2011; **196**: 1332–8. doi: <https://doi.org/10.2214/AJR.10.5698>
 22. Liu S, Sheng H, Shi H, Li W, Fan J, He J, et al. Computed tomography portography of patients with cirrhosis with normal body mass index: comparison between low-tube-voltage CT with low contrast agent dose and conventional CT. *Medicine* 2018; **97**: e13141. doi: <https://doi.org/10.1097/MD.00000000000013141>
 23. Iyama Y, Nakaura T, Yokoyama K, Kidoh M, Harada K, Tokuyasu S, et al. Impact of knowledge-based iterative model reconstruction in abdominal dynamic CT with low tube voltage and low contrast dose. *AJR Am J Roentgenol* 2016; **206**: 687–93. doi: <https://doi.org/10.2214/AJR.15.14518>
 24. Araki K, Yoshizako T, Yoshida R, Tada K, Kitagaki H. Low-voltage (80-kVp) abdominopelvic computed tomography allows 60% contrast dose reduction in patients at risk of contrast-induced nephropathy. *Clin Imaging* 2018; **51**: 352–5. doi: <https://doi.org/10.1016/j.clinimag.2018.05.027>
 25. Svensson A, Thor D, Fischer MA, Brismar T. Dual source abdominal computed tomography: the effect of reduced X-ray tube voltage and intravenous contrast media dosage in patients with reduced renal function. *Acta Radiol* 2019; **60**: 293–300. doi: <https://doi.org/10.1177/0284185118783213>
 26. Nakaura T, Nagayama Y, Kidoh M, Nakamura S, Namimoto T, Awai K, et al. Low contrast dose protocol involving a 100 kVp tube voltage for hypervascular hepatocellular carcinoma in patients with renal dysfunction. *Jpn J Radiol* 2015; **33**: 566–76. doi: <https://doi.org/10.1007/s11604-015-0457-7>